IIETA International Information and Engineering Technology Association
Advancing the World of Information and Engineering

Annales de Chimie - Science des Matériaux
Vol. 49, No. 6, December, 2025, pp. 669-684
Journal homepage: http://iieta.org/journals/acsm

Finite Element Simulation for Reducing Stress Concentration Around a Central Hole Using Optimized Adjacent Hole Designs

Yasir Hassan Ali[1], Abdoulhdi A. Borhana Omran[2], Zainab Mohamed Tahir Rashid[1], Emad Toma Karash[3*]

[1] Mechanical Engineering Techniques, Polytechnic College Mosul, Northern Technical University, Mosul 41001, Iraq
[2] Department of Mechanical and Mechatronic Engineering, Faculty of Engineering, Sohar University, Sohar P C-311, Oman
[3] Department of Fuel and Energy Engineering Technologies, AL-Amarah University, Amarah 62001, Iraq

Corresponding Author Email: emadbane2007@ntu.edu.iq

https://doi.org/10.18280/acsm.490609

Received: 10 September 2025
Revised: 17 October 2025
Accepted: 24 October 2025
Available online: 31 December 2025

Keywords:
intensity stress, aluminum alloy, von Mises stress, steel, finite element

ABSTRACT

A discontinuity and higher stress are experienced at the hole's edge when a circular hole is placed into a rectangular composite plate. The component will fail where the concentration of stress is highest. A cost-effective and lightweight solution is to create additional adjacent holes and use numerical methods and simulations to determine their positions and diameters. The objective of this study is to find the ideal locations, sizes, and forms of auxiliary slots in steel (AISI 4130) and aluminum (AA7075-T6) sheets using numerical techniques. SolidWorks was used to construct the models, and ANSYS was used to analyze the stress and deformation under different loads. The goal of the study is to improve the mechanical performance of the sheets and reduce the accumulation of stress near the central slot. In order to strengthen structural integrity, expand safety margins, and lessen stress concentrations, it also looks at the symmetrical distribution of slots in relation to existing slots. This improves the sheet's longevity under a variety of loading scenarios. The results showed that geometric adjustments to the hole distribution significantly improved the mechanical performance of both AISI 4130 steel and AA7075-T6 aluminum alloy. Both metals showed a progressive decline in ultimate stress values, indicating that the symmetrical hole design increases load transfer and reduces stress concentration. Aluminum shown a higher sensitivity to geometric adjustments, with a stress reduction of up to 22.5% compared to 18.6% for steel. Steel, on the other hand, demonstrated less stress dispersion and greater mechanical stability due to its strength and resistance to deformation. Statistical analysis revealed significant differences between the models, with the better design increasing structural efficiency by almost 25%. For applications requiring stiffness and long-term stability, steel is therefore considered more reliable; nonetheless, aluminum permits more design flexibility.

1. INTRODUCTION

Stress concentration problems in mechanical components are one of the main factors affecting the durability and efficiency of engineering systems. Small holes or flaws in the material can significantly raise local stress and possibly cause an early collapse. When exposed to tensile or bending stresses, the center hole in panels or structural parts is one of the most susceptible locations to stress concentration. Reducing stress concentration through technical solutions is necessary to improve durability and performance. One such strategy is to drill auxiliary or side holes near the core hole [1-4]. These additional holes should extend the component's service life and reduce the likelihood of mechanical failure by reducing high-stress areas and more evenly distributing pressures. Finite element analysis (FEA) simulation enables the accurate study of stress distribution and the evaluation of the design impact of side holes prior to the actual design being carried out. This approach eliminates the need for costly physical testing and enables the design to be improved gradually and scientifically [5-7]. There are several important ways to deal with stress concentration on the edge of a hole, including: Fillets ought to be served first. Fillets along the edge of a hole reduce the sudden change in form and concentration of stress. It has been demonstrated that this approach improves stress dispersion. Second, the stress concentration can be decreased by reshaping the diamond-shaped hole into a circular one. According to simulations, compared to a diamond shape, a circular design can lower stress by as much as one-third. Thirdly, employing materials that are reinforced: Better stress distribution is achieved by reinforcing the area around the hole using high-stress-resistance materials. Research indicates that the use of reinforced materials significantly reduces stress concentration [8-10]. The concentration of tension close to a hole's edge must therefore be addressed in engineering design. Using finite element simulation and implementing the previously mentioned strategies can improve component performance and service life.

2. REVIEW OF PREVIOUS STUDIES

Some of the most important earlier studies in this field that addressed the control of stress concentration around holes in sheets and were of the highest scientific grade are included below: Quantifying and analyzing the stress distributions around a circular hole reinforced with infinite aluminum sheets under uniaxial strain was the aim of the project [11]. The effects of the ring dimensions, the reinforcing ring materials (aluminum, brass, and mild steel), and the ratio of the sheet's and the ring's Young's modulus on the stress concentration factor were also investigated. The findings were compared to previous studies and Gurney's analytical theories. The results showed that utilizing metal rings to support the hole significantly reduces the stress concentration at the hole's edge and that the SCF value was affected by the kind of material, ring size, and the Young's modulus ratio of the sheet to the ring. The results showed how effective reinforcing rings are at reducing the concentration of stress in metal sheets, which largely validated Gurney's theories. The impact of perforations on stress distribution in metal and composite sheets has been examined in a number of studies, with particular attention paid to material characteristics, perforation distribution and form, and numerical analytic techniques. The impact of a central perforation in titanium and aluminum sheets under uniform axial tension (1000 N) at four different thicknesses was examined by Burjes et al. [12], who found that the stress concentration coefficient (SCF) values were very consistent between analytical methods and numerical simulations, with the largest variance at a thickness of 10 mm. This demonstrated how well the finite element method works for quickly and precisely estimating stresses. Liu et al. [13] investigated the impact of sheet thickness, Poisson's ratio, and stress ratio on the three-dimensional stress distribution surrounding a circular perforation and showed how they significantly affected the SCF, especially close to the surface. Subsequent research revealed the impact of abrupt loadings on perforated sheets [14], demonstrating an increase in stress concentrations and failure risk. Sivák et al. [15] examined the impact of perforation depth and width, demonstrating that larger perforations result in higher stress concentrations and lower material strength. Installing fasteners around holes decreases stress concentration and increases material stiffness, according to a study [16]. A study [17] that looked at the effects of the mechanical properties of materials found that mechanical quality gradients reduce the concentration of stress close to holes. While the XFEM approach in reference [18] showed that adding surrounding holes might reduce SCF by up to 35%, [19, 20] showed that adding nearby holes can reduce stress concentration around the primary hole by 20–25%. The design of neighboring holes in spherical pressure vessels reduces SCF by up to 40%, according to a study [21]. A study comparing the examination of steel and composite plates revealed that, with the exception of shear stress, which increased by a comparable percentage, the stresses in composite materials are roughly one-third lower than in steel [22]. Compared to circular holes, oval holes lower stress and strain concentration, according to a study [23]. Research has demonstrated that gradually increasing the material stiffness away from the perforation lowers the stress-strain coefficient (SCF) in materials having mechanical gradients (FGMs), as covered in references [24-28]. Stress-strain distribution and failure indices are influenced by the direction and gradient of Young's modulus, and the SCF is reduced by using FGM layers with suitable thicknesses and distributions. Lastly, a study [29] showed that when two perforations are present, the radial distribution of perforations in sheets under biaxial pressures concentrates stress, with the largest stress concentration under pure shear circumstances. This emphasizes how crucial perforation placement and size design are for enhancing sheet metal and composite performance and lowering failure rates. All of these studies demonstrate that employing materials with graded mechanical properties, altering the shape and distribution of perforations, and using numerical analysis tools like FEA and ANSYS are efficient methods for lowering stress concentration and boosting resistance to deformation and structural failure. Additionally, it was shown that the stress concentration coefficient increases with the number of holes, requiring the engineering design to incorporate an additional safety factor. The work's objective is to develop a finite element model that mimics the graded aluminum-copper alloy's progressive forming process by precisely predicting forces and stress-strain distributions using ABAQUS software [30]. The model was able to predict the material's behavior during forming, according to the results; nevertheless, more work is needed to increase its accuracy. As a result, better manufacturing procedures will yield stronger and more efficient goods. Finally, several studies have demonstrated the value of ANSYS in the analysis and design of complex assemblies and structures, especially in the fields of mechanical, civil, and aerospace engineering. Researchers have utilized the application to simulate stresses, strains, and deformations in a variety of components, enabling an extremely accurate evaluation of engineering and mechanical performance prior to actual manufacturing. Some of the references that have addressed this use are these articles. The results of these studies have demonstrated a high level of accuracy in predicting the behavior of materials and buildings under various loads [31-33]. The most important findings of earlier research indicate that the concentration of stress around holes in sheet metal is affected by the thickness, diameter, depth, and geometry of the holes as well as boundary conditions and abrupt loading. The thickness of the sheet and the reinforcing ring are additional crucial elements. While some studies [11, 16, 25] have demonstrated that the presence of nearby holes or a specific hole arrangement can reduce stress concentration by as much as 40%, other studies [18-21, 29] have demonstrated that the addition of metal rings or fasteners around holes significantly reduces stress concentration.

Additionally, studies have demonstrated that, in comparison to homogeneous materials, the use of finite-grade materials (FGMs) [24, 27, 28] lowers the SCF near the hole edge, particularly when the proper Young's modulus gradient is used. Studies show that the distribution of stress is strongly influenced by the hole's form [23], with oval holes having a lower failure rate than circular ones. Lastly, a number of studies [12, 22, 30] have shown how effective it is to simulate stresses, strains, and deformations using ANSYS software and the finite element approach. By accurately predicting how materials and structures will respond under different loads, this method enhances mechanical and engineering performance reliability and permits design optimization before actual manufacture.

3. THE OBJECTIVE OF STUDY

In this work, neighboring holes of varying geometric forms and sizes are designed around a center hole in sheet metals composed of different metals in order to assess and reduce stress concentration around the central hole. The primary goal of the study is to assess how these geometric changes affect the distribution of stresses, strains, and deformations in the sheets under bending and tensile loads. Modeling is done with Solid Works, and finite element analysis (FEA) simulations are done with ANSYS. The outcomes are carefully examined. The best design that reduces stress concentration and improves the sheet metal's strength and structural integrity is found by comparing the performance of several models.

4. DESIGN MODELS

4.1 Model shapes and dimensions

Figure 1 shows various geometric models with their dimensions, four for AA7075-T6 aluminum alloy and four for steel. They all relate to a mechanical part containing central holes of varying shapes to reduce weight and study their effect on stress concentration. A detailed description of each model is provided below.

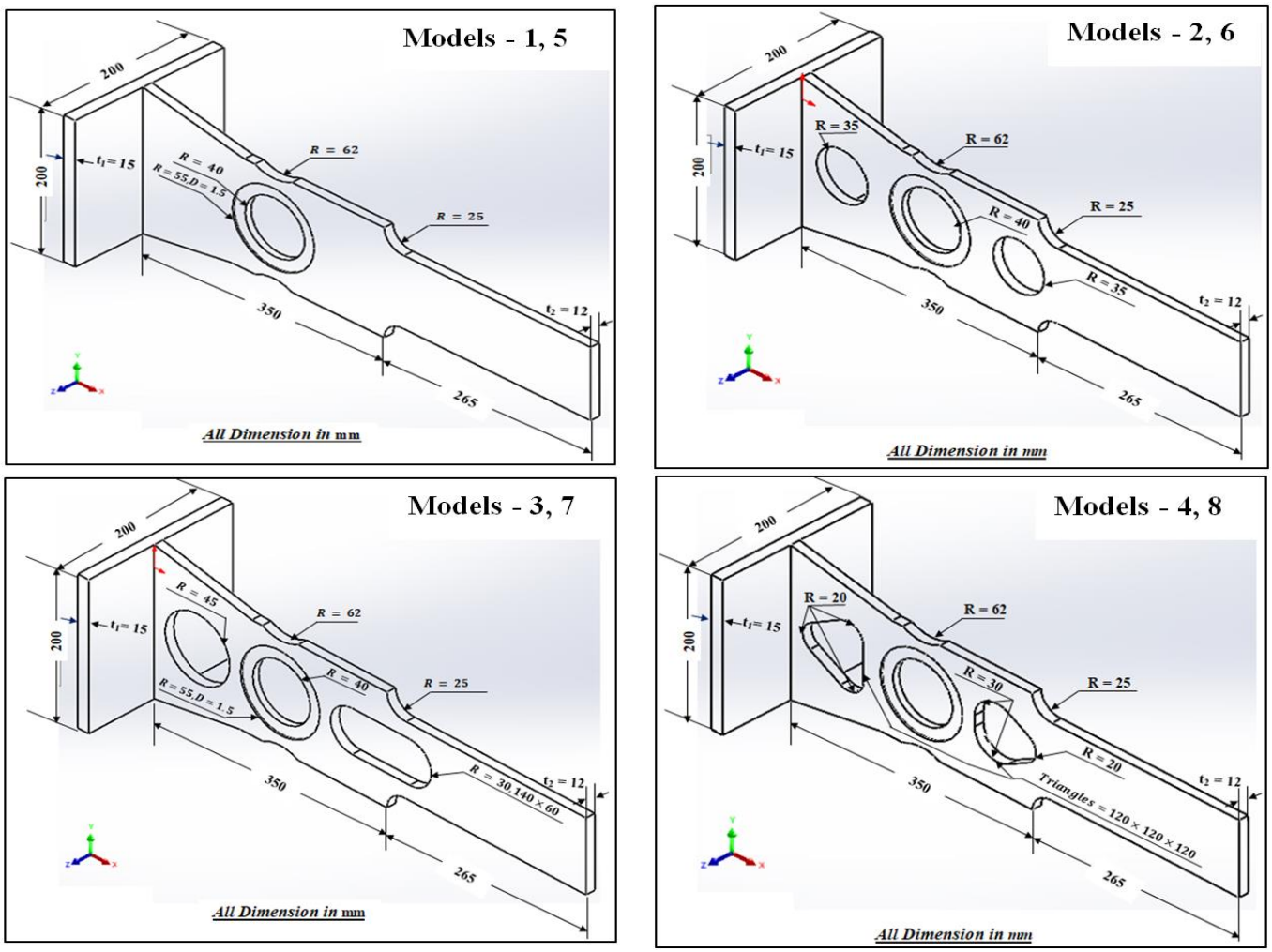

Figure 1. Geometrical optimization of perforated plates for stress reduction using different hole configurations

Model 1, 5 - It has a single circular hole in the center with a large diameter (R = 40mm).

The design is simple and symmetrical about the longitudinal axis.

Overall dimensions: Total length 615 mm, base width 200 × 200 mm.

This model serves as a comparison because it lacks additional holes. It is the simplest model for stress analysis around a single hole.

Models 2 and 6 were designed with the same dimensions as Model 1, but with two holes on either side of the central hole, each with a radius of 23 mm. These holes were created to modify the geometric and structural characteristics of the two models. Distributing stress and lessening its concentration around the main hole is the aim of this improvement. With the same body length and width, the overall measurements are comparable to those of the previous model. But the extra aperture modifies the distribution of stress.

Model 3, 7 - It has three holes with varying dimensions (R = 40 mm for the center, circle R = 45 mm for the corners, oval R = 30, length = 140 mm), two of which are circular and the third is oval. The model's goal is to investigate how the quantity and spacing of holes affect bending and tensile stresses. Compared to the first two models, the design is more intricate, and when homogenous materials are used, a more uniform stress distribution is anticipated.

Model 4, 8 - Alongside the primary circular entrance, there are two elliptical or oblique openings. In terms of geometry,

this design is the most complicated example. Since oval apertures are anticipated to lower maximum stresses, the objective is to assess the impact of opening form (circular vs. elliptical) on stress concentration. With the exception of the opening shape, the overall dimensions are the same as those of the earlier variants.

4.2 Materials used

Table 1 contrasts the mechanical and physical properties of AISI 4130 steel and AA7075-T6 aluminum alloy, two materials commonly utilized in the building of automobiles, railroads, and aircraft. According to the statistics, AISI 4130 steel's high hardness and remarkable tensile strength allow it to withstand heavy loads and difficult mechanical conditions. However, the aluminum alloy AA7075-T6 is ideal for applications that require less mass without sacrificing strength and stiffness since it is lighter and has an excellent strength-to-weight ratio. As the table also shows, both materials are ductile, but AISI 4130 steel is more durable, whereas AA7075-T6 aluminum alloy is more formable and machinable and has an acceptable level of stress and strain resistance. This comparison aids engineers and researchers in choosing the best material for advanced structural designs based on weight and mechanical performance requirements.

Table 1. Comparing AISI 4130 steel and AA7075-T6 aluminum alloy, including their physical and mechanical properties [34-38]

No.	Property	AISI 4130 Steel	AA7075-T6 Aluminum Alloy
1	Density (kg/m³)	7850	2810
2	Young's Modulus (GPa)	207	72
3	Shear Modulus (MPa)	80	26.9
4	Poisson's Ratio	0.30	0.33
5	Ultimate Tensile Strength (MPa)	660	572
6	Elongation at Break (%)	21.5	11
7	Brinell Hardness (HB)	217	150
8	Fatigue Strength (MPa)	310	159
9	Yield Tensile Stress (MPa)	560	503
10	Yield Shear Stress (MPa)	320	290

4.3 Mesh

Figure 2 shows the mesh type and the locations of roughness and smoothness in the various models, four of which are for steel and four of which are for the aluminum alloy AA7075-T6. Since they are perfect for representing complex geometric structures with curved corners and circular apertures, tetrahedral meshes, or three-dimensional tetrahedral elements, were used in all models. These parts don't require complex geometric division and provide excellent distribution flexibility over the model. The mesh's density is not constant throughout the model but rather fluctuates based on the type of area when the mesh size gradient concept is applied, as demonstrated below:

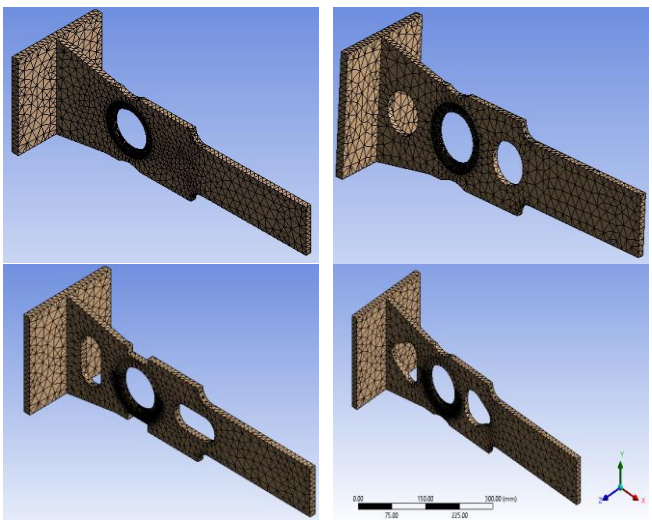

Figure 2. Mesh distribution showing fine and coarse regions for steel and AA7075-T6 aluminum alloy models

The mesh is coarse in areas far from openings or non-critical edges because of the consistent and mild change in stress and strain there; larger elements can be utilized there without compromising the accuracy of the analysis. While the total number of pieces and computation time are reduced, only the most crucial areas of accuracy are preserved. Because of this, the mesh in the four models is not uniformly dense; instead, it is produced via a slow, hybrid process that consists of: fine mesh surrounding high-stress areas, such as apertures. In remote locations (where stress is low and stable), coarse mesh.

The rationale for choosing this distribution was to achieve the best possible balance between computational accuracy and numerical solution speed in ANSYS. Although the number of elements enhances accuracy, so does the number of equations and solution time. In order to reduce computation costs without compromising the accuracy of the final results, the focus was on lowering the elements in areas where load and stress fluctuate rapidly while maintaining their size in other areas.

Due to the concentration of stress in the holes and section transition zones, a high-density mesh was used for finite element simulation. When switching from a coarse mesh (element size = 8 mm) to a medium mesh (5 mm), the von Mises maximum stress value varied by 12–18%, however the findings changed by only 2.5% when employing a very tiny mesh (3 mm), showing convergence with the numerical solution. Additionally, the models demonstrated that with mesh optimization, the overall distortion dropped from 0.84 mm to 0.79 mm, validating the choice of an adaptive mesh to enhance element distribution without appreciably increasing the number of elements. In contrast to triangular components, which saw distortion of up to 14% close to the holes, quadrilateral elements in flat areas decreased element distortion to less than 5%. To guarantee the consistency of the numerical results and reduce rounding error, the Aspect Ratio was also maintained between 1 and 3. Thus, the optimal balance between the precision of the results and the computing

effort is achieved by selecting a grid that is centered around the holes and a grid that is intermediate in the remainder of the body.

4.4 Forces applied

The mechanical and geometric values of eight models four of which were made of AISI 4130 steel and four of which were made of AA7075-T6 aluminum that were subjected to numerical analysis are displayed in Table 2. Weight, volume, and center of mass (center) of each model are included, along with the forces and moments employed in the numerical test (torque of 20 kN/mm and tensile forces of 100 and 30 kN). The table also describes the number of nodes and elements for each model and the mesh used in the numerical analysis. The values vary according to the material properties and model shape.

Figure 3 shows how eight distinct models—four upper models for the AA7075-T6 and four lower models for the AISI 4130 were subjected to static loading conditions. Force 1 varies according to the weight of the model, while Force 2 is equal to 100 kN for all models, Force 3 is equal to 30 kN for all models, and the torque (Moment) is 20 kN.mm. The left end of each model was fixed by a fixed support, while the right end was exposed to graded tensile forces. Examine the impact of model form and material type on the mechanical response (stress, displacement, and transmitted moment) under identical loading conditions since the figure illustrates how the order and direction of forces vary between models.

Table 2. Shows the geometric and loading properties of simulated models of AA7075-T6 and AISI 4130 alloys

Metal	Model	Centroid (X, mm)	Volume (m^3)	Weight (Kg)	Force – 1 (N)	Force – 2 (KN)	Force – 3 (KN)	Torque (KN. mm)	Nodes	Elements
AA7075-T6	I	156.89	$1.4722*10^6$	4.1369	40.58	100	30	20	37088	22659
	II	155.64	$1.3799*10^6$	3.8774	38.40				34957	21322
	III	151.46	$1.3555*10^6$	3.8089	37.37				36518	22108
	IV	155.37	$1.342*10^6$	3.771	36.99				39685	24445
AISI 4130	V	156.89	$1.4722*10^6$	11.557	113.37				37088	22659
	VI	155.64	$1.3799*10^6$	10.832	106.26				34957	21322
	VII	151.46	$1.3555*10^6$	10.239	100.44				36518	22108
	VIII	155.37	$1.342*10^6$	10.637	104.35				39685	24445

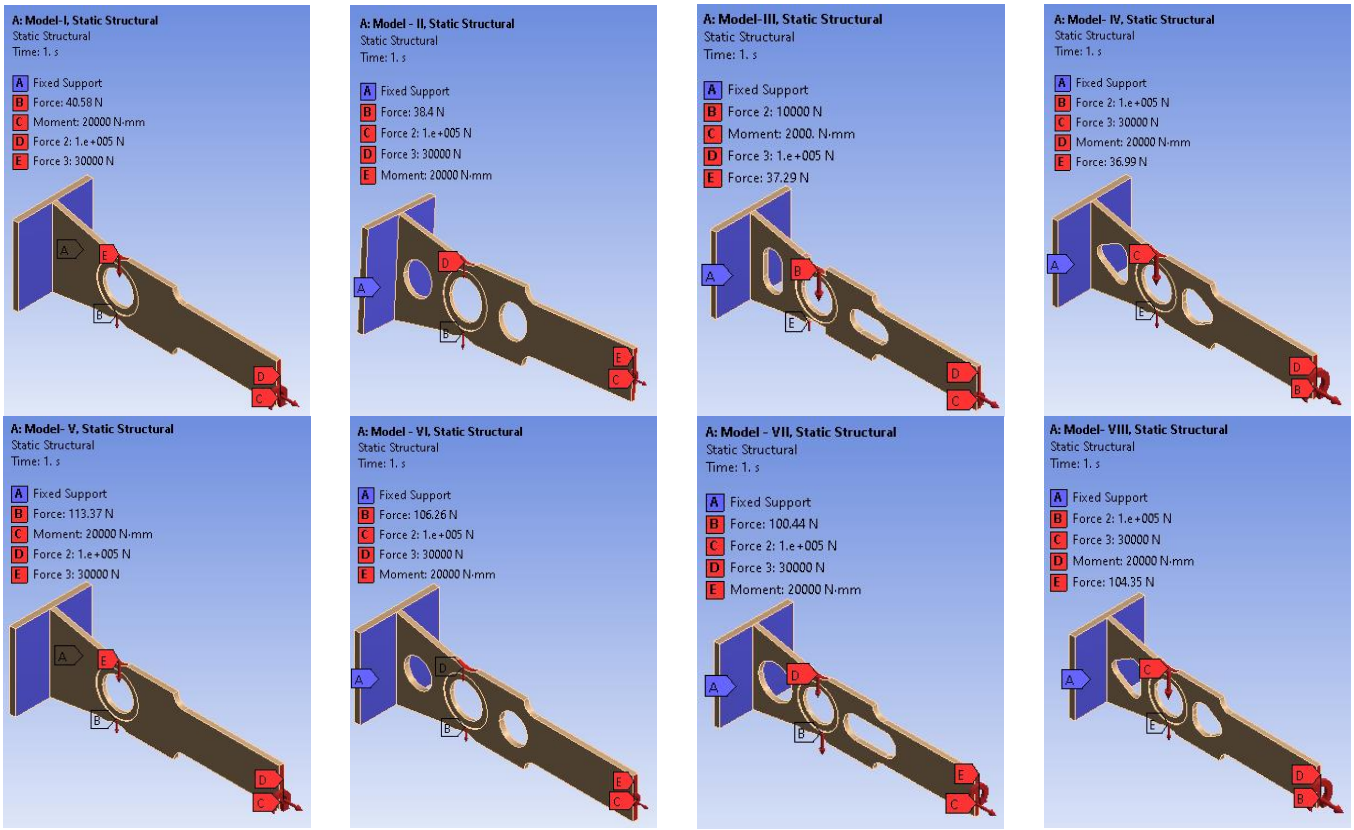

Figure 3. Shows the loading and clamping locations for the AISI 4130 and AA7075-T6 geometric models in static analysis

5. RESULTS AND DISCUSSION

5.1 Von Mises stress results

Figure 4 shows eight models analyzed using ANSYS under static structural analysis. Von Mises stresses were distributed across models containing holes of various shapes or arrangements.

The first four are aluminum alloy, while the second four are steel alloy.

A brief, detailed description of each group is provided below:

The First Four Models AA7075-T6 aluminum alloy:

The areas of greatest stress surrounding the holes' edges, especially at the center hole or the points of contact with the edges, are shown by the red hue. The form and arrangement of the holes affect the maximum stress values, which vary from about 440 to 640 MPa. A single hole results in a dramatic concentration of stress, as demonstrated by the first model, which displays stress concentration at the top of the center hole. Because the load is more evenly distributed in the middle, the second and third models show that lateral perforations lessen stress there. The opposing hole arrangement lowers the overall stress, as evidenced by the fourth model's optimal stress distribution and lower maximum values.

The presence of additional holes or a symmetrical arrangement leads to better stress distribution and reduced deformation in the central hole, improving the performance of the part under load.

AISI 4130 steel:

Due to steel's stronger mechanical qualities, the maximum stress values are higher than those of aluminum (up to about 760 MPa). Near the holes, especially along the inner margins of the core hole, the areas of greatest stress continue to be focused. In models with more than one hole, where stress concentration is lower, the distribution is more uniform despite the larger values. With a more evenly distributed tension and no obvious stress concentration, the final steel model exhibits the finest mechanical response. Because of its greater strength, the material can withstand stress values that are higher than those of aluminum, and the balanced distribution of holes lowers the possibility of local failure.

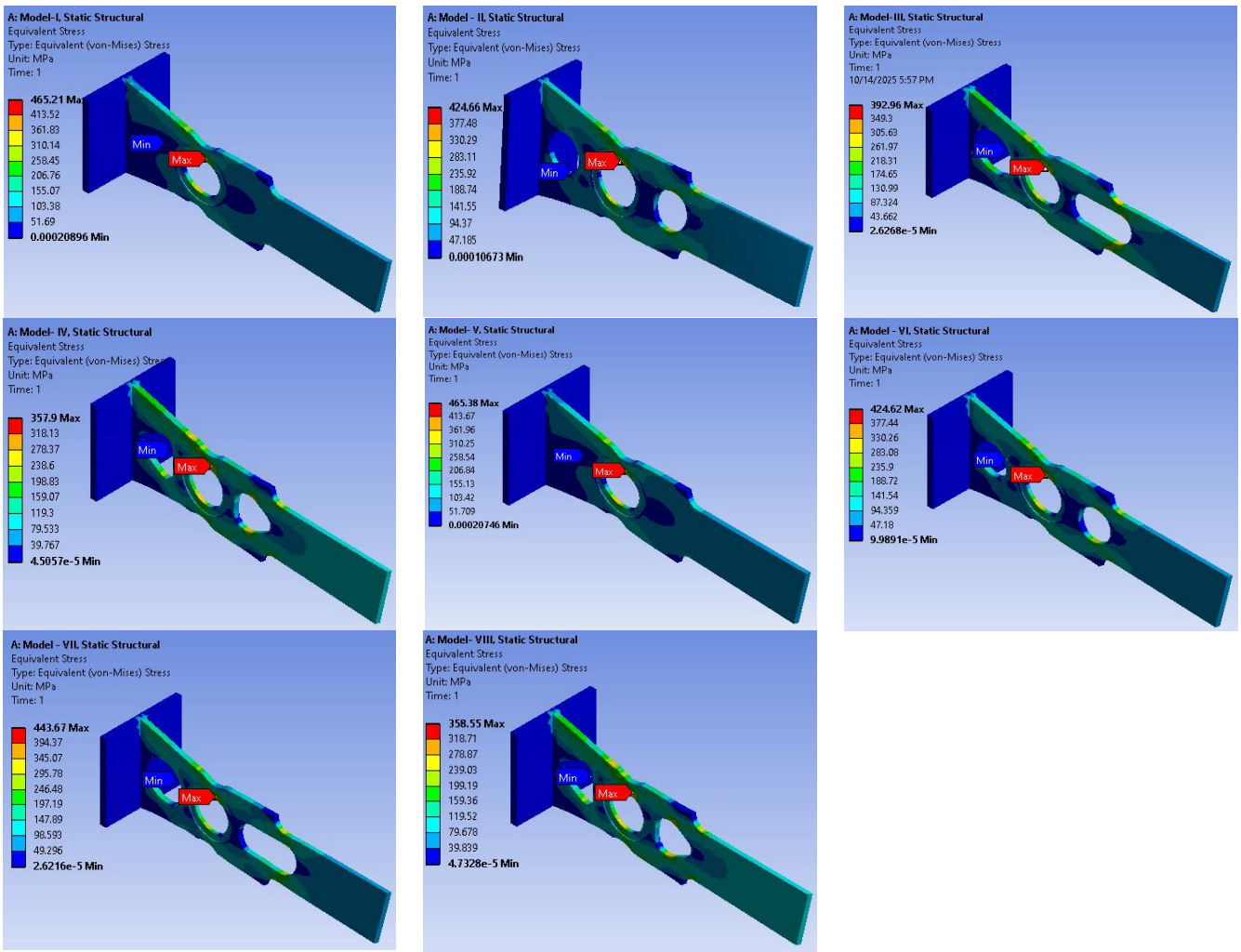

Figure 4. Distribution of von Mises stress results for aluminum and steel alloy models (I–VIII) under static loading conditions using ANSYS simulation

The following determines the stress reduction ratios according to the von Mayes equation for each model, compared to the reference model for each alloy:

Steel alloy AISI 4130 (Models I–IV, Reference I = 465.21 MPa), II: ≈ 8.7% reduction; III: ≈ 15.6% reduction; IV: ≈ 23.1% reduction. AA7075-T6 aluminum alloy (Models V–VIII, Reference V = 465.38 MPa), VI: ≈ 8.7% reduction; VII: ≈ 4.7% reduction; VIII: ≈ 22.9% reduction.

Steel exhibits a continuous gradual reduction from the middle models (~8.7–15.6%) to the lowest model (~23.1%), while aluminum maintains a greater stability for the middle models (~4.7–8.7%) before decreasing to the last model (~22.9%).

Comparison results with the von Mises stress theory for the eight models indicate that all models operate within the elastic range of both AA7075-T6 aluminum alloy and AISI 4130 steel under applied loading. For aluminum, which has a yield stress of 503 MPa, the maximum von Mises stress values ranged

between 440 and 465 MPa, meaning the models operate at ≈87–93% of the yield limit. Model 4 performed the best and achieved the largest stress reduction (~22.9%) because of improved load distribution and reduced stress concentration in the holes. While keeping an average safety rating (≈91–92%), models 2 and 3 fared much better than reference model 1, which had the highest stress concentration. The greatest von Mises stress values for steel in the reference model varied from 465 to 465.21 MPa, with a yield stress of 560 MPa. Model II, Model III, and Model IV all showed a progressive decline, with Model II's von Mises stress values being 8.7%, 15.6%, and 23.1%, respectively. As a result, the stress ratio for each model ranges from 77 to 83% of the yield limit. With the lowest stress concentrations and the optimum stress distribution, Model IV ensures structural integrity and lowers the possibility of local deformation.

These findings show that the von Mises stress distribution and stress concentration in steel and aluminum may be directly influenced by the number and arrangement of holes, as long as all models remain within a safe elastic range that does not exceed the yield limit of each material. However, aluminum approaches the yield limit more closely than steel, therefore careful engineering design is required to maximize the safety margin at higher concentration points.

5.2 Maximum shear stress results

Figure 5 shows the maximum shear stress results obtained for all models using ANSYS software and the finite element method for static structural analysis. The first four models are aluminum alloy, and the last four are steel alloy, with different hole arrangements and shapes.

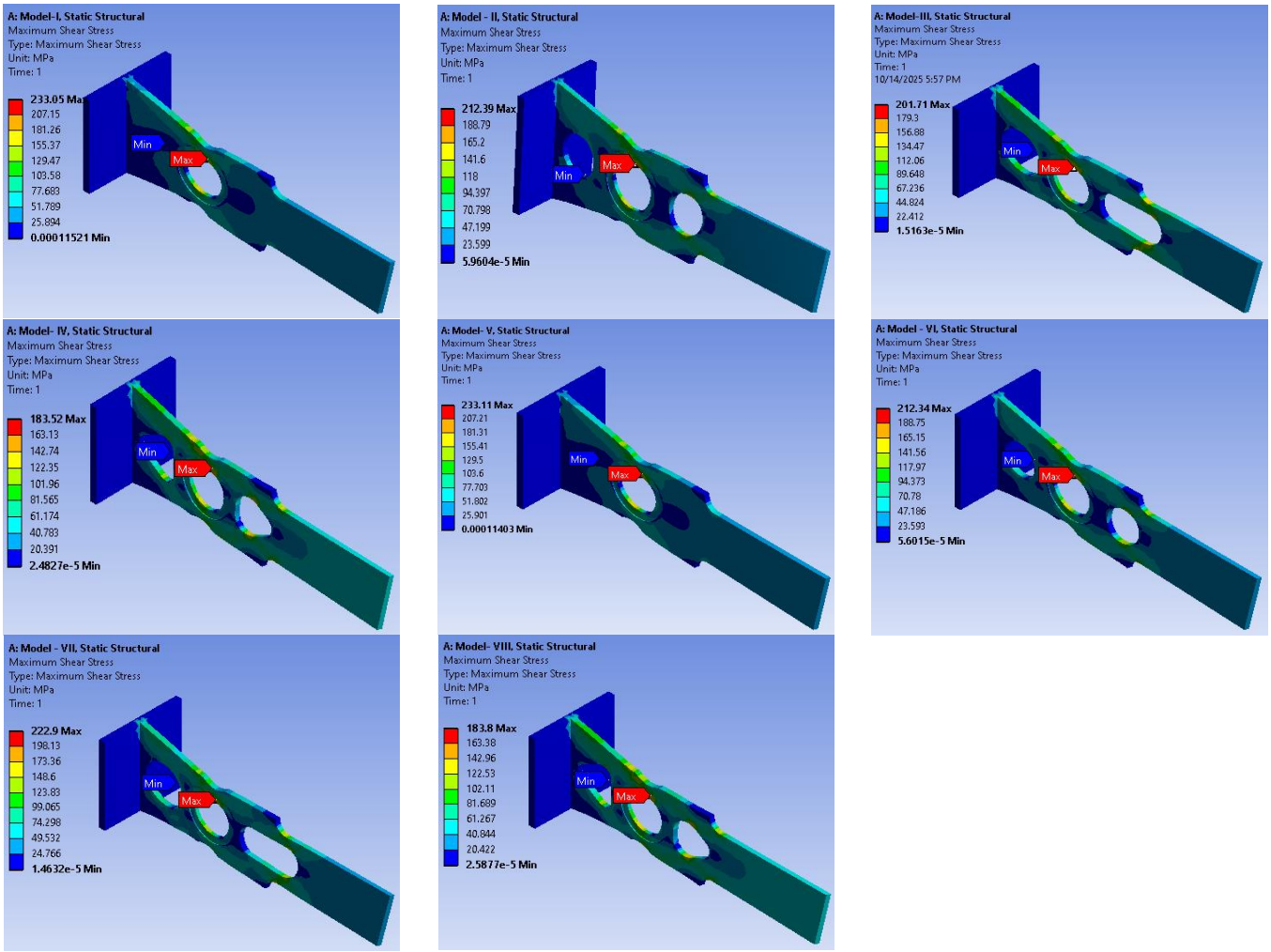

Figure 5. Distribution of maximum shear stress for aluminum and steel alloy models (I–VIII) under static loading conditions using ANSYS simulation

The following is a detailed and analytical description of each group:

The First Four Models – Aluminum Alloy (Models I–IV):

Maximum shear stress values range approximately from 180 to 223 MPa. In all models, the maximum stress concentration (red) is evident around the edges of the central hole, particularly at the top and bottom.

Due to stress concentration at the single central hole, the first model showed the maximum stress (~223 MPa), suggesting inadequate load dispersion. The second model reduced stress and mitigated the central concentration by shifting the stress distribution towards the lateral holes. Because of the lateral holes, the third model displayed a more balanced distribution, with peak values dropping to roughly 190–200 MPa. The effectiveness of symmetry in load distribution and lowering local stresses was confirmed by the fourth model's symmetrical hole design, which produced the lowest ultimate stress. Increasing the number of holes or placing them symmetrically enhances the design's resistance to failure while also improving stress distribution and lowering

peak values. Improved steel is used in the latter two variants (V–VIII). Because of the steel's high hardness, maximum ultimate stress values are somewhat greater, ranging from roughly 220 to 230 MPa. Model V: There is a lot of stress close to the central hole's edge. With a larger range of values, stress concentration behaves similarly to aluminum. Model VI: As the stress distribution over the lateral holes improves, maximum values start to decline. Model VII: Has a maximum stress of about 223 MPa and a more uniform distribution. Sharp tension concentration is lessened by the symmetrical design. Better mechanical stability for steel in this form is shown by Model VIII, which has the best ultimate stress distribution and the lowest stress concentration. Although the ultimate stress values are relatively high, the steel can easily withstand them due to its high strength. The presence of symmetrical or geometrically distributed holes also reduces weak points and increases structural rigidity.

The following is the percentage decrease in maximum shear stress for each model compared to the reference model for each alloy:

Steel alloy AISI 4130 (Models I–IV, Reference I = 233.05 MPa); II: ≈ 8.7% reduction; III: ≈ 13.5% reduction; IV: ≈ 21.3% reduction.

AA7075-T6 aluminum alloy (Models V–VIII, Reference V = 233.11 MPa); VI: ≈ 8.9% reduction; VII: ≈ 4.4% reduction; VIII: ≈ 21.1% reduction.

Steel exhibits a continuous gradual reduction from the middle models (~8.7–13.5%) to the lowest model (~21.3%), while aluminum maintains a greater stability for the middle models (~4.4–8.9%) before decreasing to the last model (~21.1%).

All models function within the elastic range of both AISI 4130 steel and AA7075-T6 aluminum alloy under applied loading, according to comparison results with theoretical maximum shear stress. Model 1 reported the highest maximum shear stress value for aluminum, which has a yield shear modulus of 290 MPa, at about 223 MPa, or roughly a 23% safety margin. At stress levels of 180 to 200 MPa, models 2, 3, and 4 performed less efficiently, with safety margins ranging from 31% to 38%. This suggests that models 3 and 4's symmetrical arrangement and better hole distribution greatly decreased stress concentration and improved structural integrity. Model 5 demonstrated a maximum stress of roughly 230 MPa for steel with a yield strength shear modulus of 320 MPa, suggesting a safety margin of about 28%. On the other hand, models 6, 7, and 8 showed enhanced load-bearing capacity due to the geometric improvements in hole distribution, with stress values ranging from 180 to 223 MPa, showing safety margins of 30% to 44%. Steel specimens frequently have a greater safety margin than aluminum, as evidenced by the eighth specimen's greatest performance, which shows the lowest stress concentration and the most uniform load distribution. This demonstrates how the geometric hole distribution enhances deformation resistance and structural integrity.

5.3 Stress intensity results

Figure 6 represents the results of a numerical simulation stress intensity using ANSYS software for different specimens under the same loading requirements. It shows the common stress intensity along the specimen.

Comparison of results in terms of the percentage reduction in stress intensity:

Comparison of models (aluminum alloy – Models I to IV):

Model I was used as a reference with 100% of the maximum stress intensity, and the relative results were as follows:

- Model I: 100% (reference – highest stress concentration).
- Model II: 91% reduction ≈ 9% compared to the reference.
- Model III: 85% reduction ≈ 15%. Model IV: 78% reduction ≈ 22%.
- Model IV appears to be the best for aluminum, achieving a significant reduction in the maximum equivalent stress of approximately 22% compared to the reference model.

Analysis and comparison of steel alloy:

- Model V (reference): Highest principal stress 461.7 MPa.
- Model VI: Stress decreased by ≈ 8% compared to the reference, indicating a relative improvement in load distribution.
- Model VII: Did not show a significant improvement (its stress was very close to the reference, + 0.9%).
- Model VIII: The best performer, achieving a minimum equivalent stress of 367.16 MPa, a 20.5% decrease compared to the reference.

Model IV was found to be the best for the steel alloy, achieving a significant decrease in the maximum equivalent stress of approximately 20.5%.

This study looks at how stress is distributed around elliptical or circular holes in an infinite plate [39]. The results of the current investigation provide support for the idea that the location and form of the hole change the distribution of stress. The computational and experimental effects of stress concentration in aluminum are investigated. The results of the investigation corroborate the theory that hole distribution and variability affect stress [40]. This study looks at a perforated steel/titanium plate and demonstrates that the von Mises stress in the core layer is reduced by about 30% when a perforated layer is present [41]. The distribution and geometry of the holes contribute to reducing stress concentration and enhancing its transmission within the structure, as evidenced by the results, which are unequivocally consistent with previous research. According to studies [42-44], the shape and spacing of the holes play a crucial role in reducing the stress concentration (SCF) by 10–25%, which aligns with the 22% and 20.5% reductions observed in contemporary models. According to study [43], bimetallic sheets with alternating layers or holes can improve load distribution and reduce von Mises stress by up to 30%, supporting the current findings for steel and aluminum. Aluminum responds more flexibly to symmetric loading and reduces equivalent stress more rapidly than steel, according to a study [45], further enhancing its superiority in reducing stress concentration. The 1.5% numerical difference found in this investigation is comparable with a study [46] that found that aluminum shows better stress distribution and a concentration reduction of about 2% when compared to steel. In comparison to more rigid materials, the study [47] also demonstrated that aluminum is more responsive to geometric changes than steel and that altering the hole's location or form greatly lowers stress intensity. The study demonstrated that there is a notable difference in stress concentration coefficients across different material types (steel versus aluminum), with SCF values being lower in softer, lighter materials like aluminum alloys [48]. It is tentatively confirmed by prior research that: (a) the effect differs between

materials/alloys; and (b) the addition or distribution of holes can either increase or decrease SCF based on size and spacing. Using two alloys (steel and aluminum), this study conducted an experimental evaluation and produced the following figures: Aluminum's maximum stress can be improved by up to about 22% (Models I–IV). Improvement in steel of up to about 20.5% (Model VIII vs. reference V). According to research in the literature, it is possible to reduce SCF by choosing the right hole geometry, albeit the degree of reduction varies depending on the material's characteristics and the micro geometry. This study offers direct and comparable quantitative values (percentages and specific numerical reductions) for the same configurations across two different materials under the same loading conditions, whereas many other studies have concentrated on the impact of a single hole shape or on general analyses of composite laminates. This provides quantifiable experimental proof of how aluminum and steel react differently when the hole distribution is changed, something that has only been suggested or partially examined in earlier research.

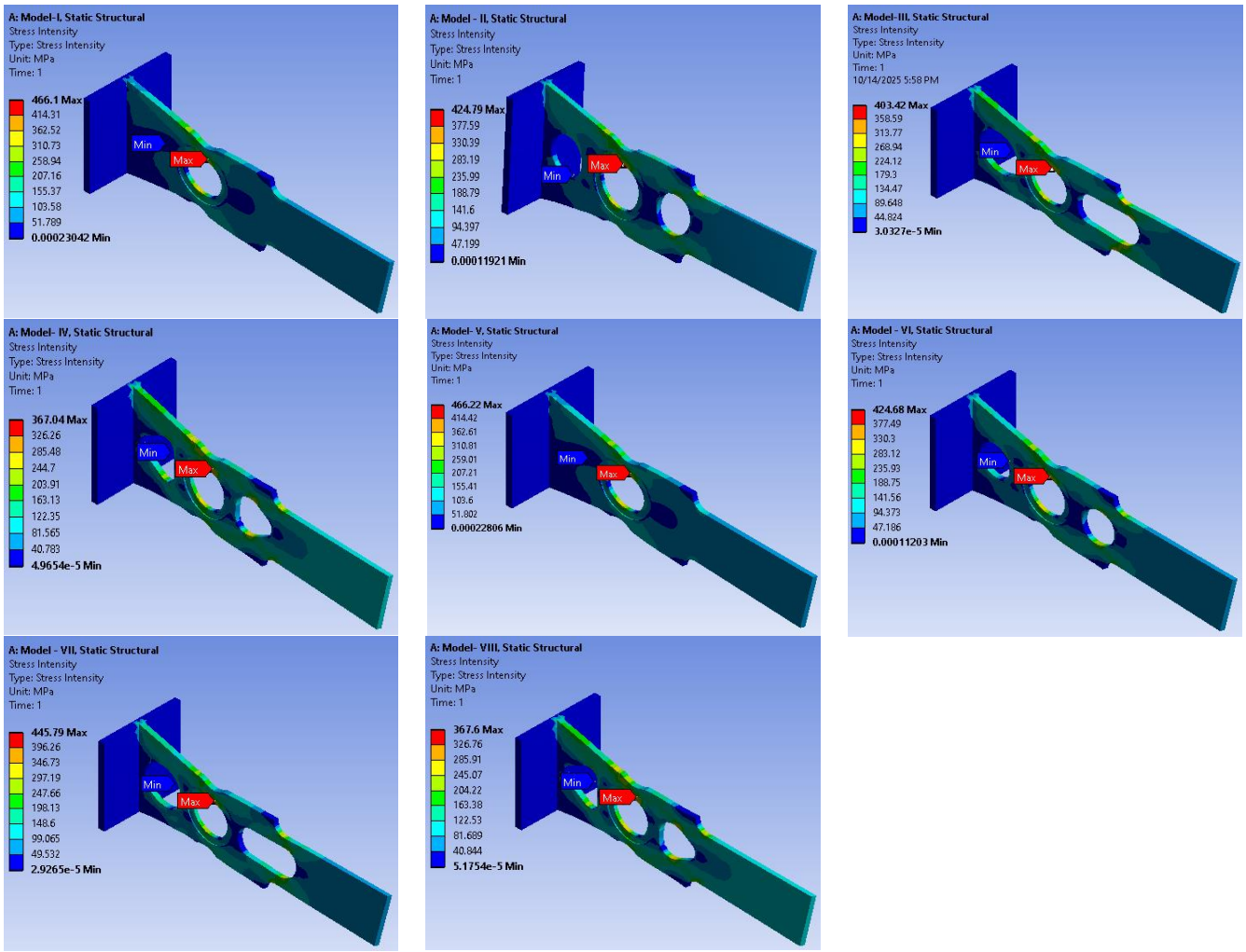

Figure 6. Comparison of the simulated stress intensity results for the eight models obtained from ANSYS static structural analysis

5.4 Equivalent elastic strain results

Figure 7 shows the numerical results of the equivalent plastic strain distribution for the eight models (four for aluminum alloy and four for steel alloy) using ANSYS Static Structural software.

Below is an analysis of the aluminum alloy models – the main elastic strain results.

Model I: The highest strain value is near the central opening. The maximum value is 0.006469 mm/mm. The areas of high strain concentration are colored red at the upper edge of the opening. Model II: The maximum strain value is lower than Model I, at 0.005935 mm/mm. The distribution is more uniform, with the concentration remaining around the opening. This indicates an improvement in stiffness compared to Model I. Model III: The maximum strain is 0.004875 mm/mm. There are less distortions since the red color is less dispersed. The stress is now distributed more equally thanks to improvements in the form or support. Model IV: 0.004498 mm/mm is the model with the lowest strain value. more even distribution of strain. most effective design in terms of resistance to deformation. A weak design was indicated by Model (V), which displayed the maximum strain of 0.00227, localized at the hole's edge. With a reduced strain and improved distribution surrounding the hole, Model (VI) recorded 0.00205. Model (VII) had a balanced stress distribution and registered 0.00214. With a homogeneous distribution and the lowest strain of 0.00174, Model (VIII) demonstrated the best mechanical performance and maximum stiffness.

Model I recorded the highest value of 0.006469 mm/mm, which serves as the basis for comparison, when the maximum primary elastic strain value of the four models was compared.

The strain value of the Model II decreased to 0.005935 mm/mm, or around 8.3% less than that of the Model I. This implies a substantial improvement in the stiffness of the model. Model III showed a lower value of 0.004875 mm/mm, or a 24.7% improvement, due to improved surface stress distribution. With the lowest maximum strain of 0.004498 mm/mm a 30.5% reduction from the first model the fourth model was the most efficient and deformation-resistant design of all.

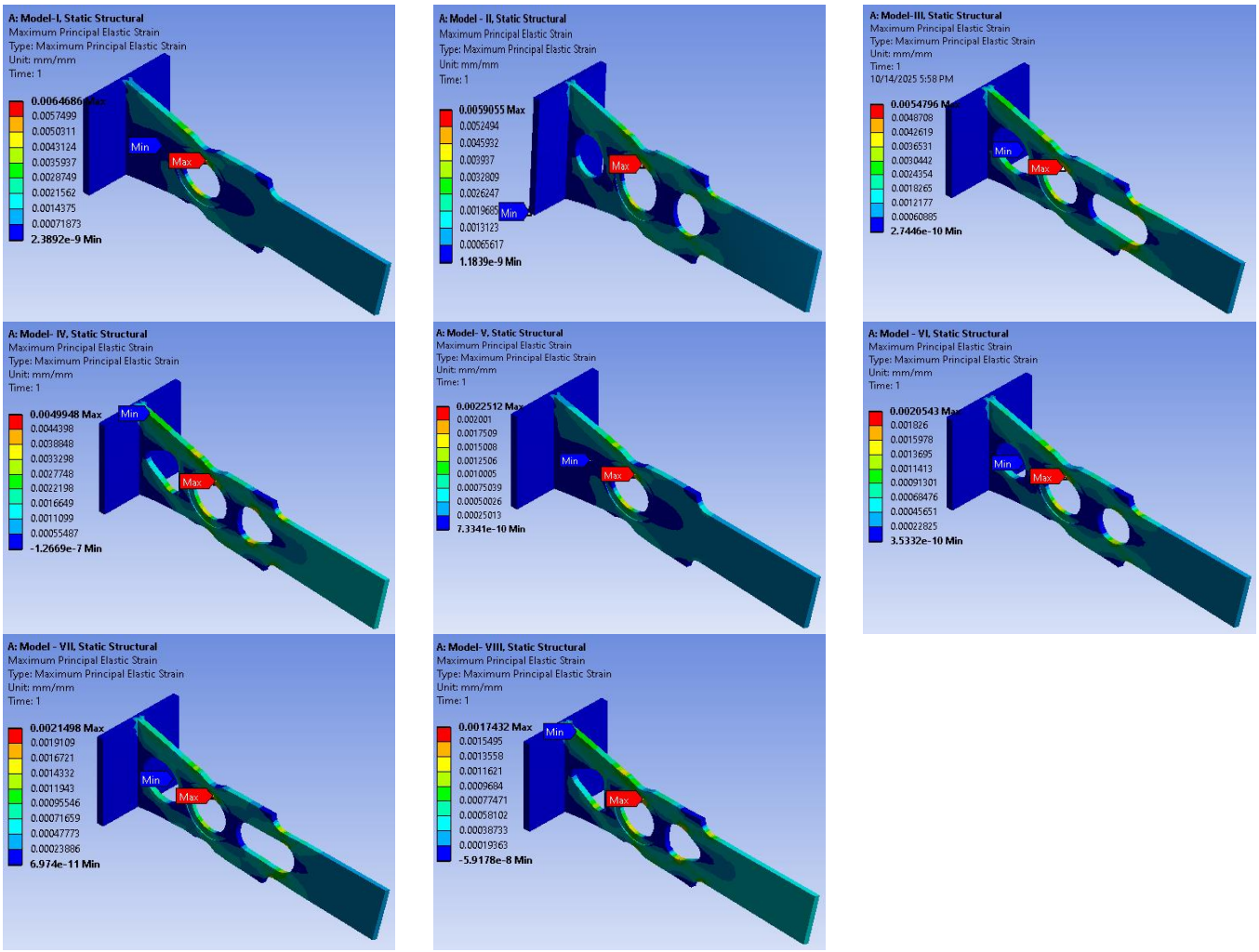

Figure 7. Analyzing the strain distribution of steel and aluminum alloy models in ANSYS simulation

The results show that the maximum primary elastic strain is reduced and stiffness is clearly improved throughout the modified models. The progressive decline from Model I to Model IV, which produced a total reduction of roughly 30.5%, shows that the improved geometric designs successfully reduced deformation concentration zones and redistributed internal stresses.

This behavior is consistent with recent discoveries in structural optimization research, which show that principal strain values are much reduced and overall stiffness is improved by using graded materials, stress-constrained design, and topology optimization. These enhancements demonstrate the need for suitable geometric refinement to reduce strain concentrations and enhance deformation resistance in components made of aluminum alloys. The results of this study are supported by this work, which demonstrates that altering the distribution of mechanical properties or adding a material gradient around the opening lowers the stress concentration factor and, consequently, the maximum strain values (which, when optimizing the distribution/design, correspond to a 24.7% and 30.5% reduction in your models) [49]. This review explains how two models (III and IV) intended to optimize the material/opening distribution result in notable reductions in maximum strain when compared to the reference model in this research [50]. It also demonstrates how topology optimization provides material/space distributions that minimize compliance and lower maximum strains/displacements. A method for explicitly constraining the first principal stress/strain in the topology optimization process is presented in this study [51]. It shows how designs that constrain the principal stress can decrease maximum stress/strain values and increase component stiffness, which directly correlates with the study's findings for shrinkages of 8.3%, 24.7%, and 30.5%.

The strain values for the steel alloy show how the design has evolved toward improved stress distribution and less deformation, ranging from the greatest in model (V) to the lowest in model (VIII). A progressive improvement in mechanical performance is demonstrated by the strain reduction between models. The drop for model (VIII) was roughly 23% less than that of model (V), 15% less than that of model (VII), and 10% less than that of model (VI). It is clear that altering the hole's shape and the distribution of materials surrounding it greatly increased its resistance to deformation.

Model (VIII) is therefore the most effective at supporting loads.

In line with Model VIII's findings, the investigation showed that adjusting the hole's shape or fortifying it with a suitable curvature gradient can lower stresses by up to 25% [52]. As the current data demonstrates, the study found that holes with modified shapes (oval or with strengthening inserts) minimize the maximum strain in comparison to circular holes [53]. According to the results, strain can be decreased by 20–30% by changing the geometric distribution of the hole and surrounding sections [54]. These results are nearly equal to the lowered strain.

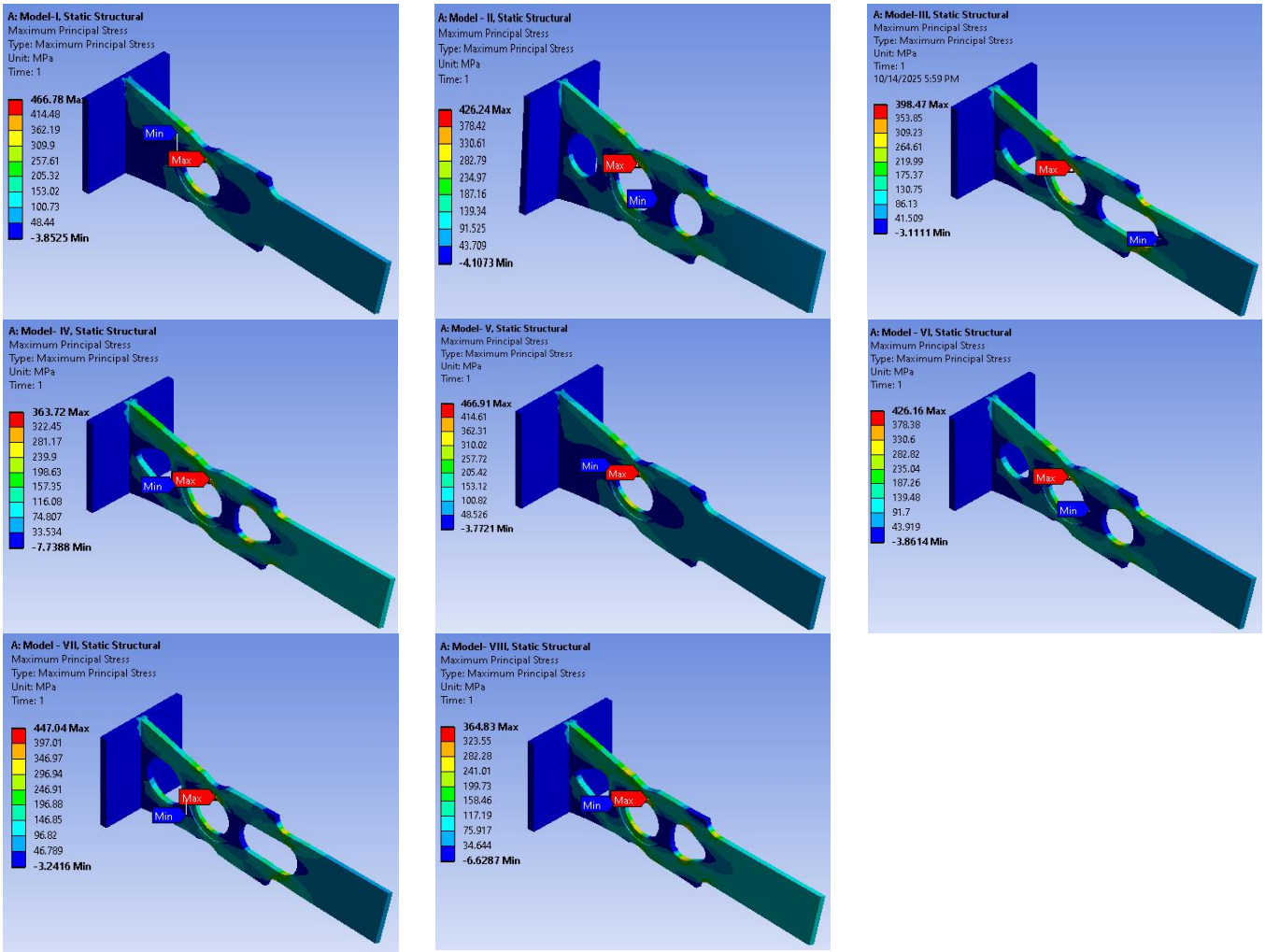

Figure 8. Principal stress results comparison for aluminum alloy and steel models in ANSYS simulation

5.5 Equivalent elastic stress results

The distribution of maximum principal stresses across eight perforated models under identical loading conditions is depicted in Figure 8. The AISI 4130 steel alloy is represented by the final four models, while the AA7075-T6 aluminum alloy is represented by the first four. The findings are displayed using colors that correspond to the highest and lowest stress levels. At the perforated edges, each model displays the place of the highest concentration of stress. The colors go from blue for the least amount of tension to red for the most. Because the perforations' shapes or arrangements differ among the models, the stress distribution differs as well. Different structural behaviors are displayed by each model, illustrating how design affects the distribution of stress.

The figure above shows the results of the numerical analysis of the ultimate stresses for eight models: four aluminum alloy models and four steel alloy models, all perforated under the same loading conditions. In the first model, the ultimate stress reached 466.78 MPa, the highest among the models, indicating a high stress concentration at the perforation edge. In comparison to the first model, the value in the second model dropped to 424.24 MPa, or around 9.1%. The third model recorded 395.47 MPa, a further decrease of nearly 15.3% when compared to the first model, indicating an improvement in load distribution. The fourth model's final stress was 361.72 MPa, the lowest stress ever measured and a drop of almost 22.5% from the first example. It is clear that every geometric modification made to the design led to a gradual decrease in the concentration of stress. The fourth model is therefore the most mechanically efficient since it has the greatest load-bearing capacity and the lowest likelihood of failure at the perforations. The steel alloy findings showed that the first model had the highest maximum stress (446.51 MPa), followed by the second model (376.16 MPa), the third model (401.04 MPa), and the fourth model (363.45 MPa), which had the lowest stress. In comparison to the first model, the stresses in the second and third models decreased by 15.8% and 10.2%, respectively. With a maximum stress reduction of 18.6%, the fourth model outperformed the others and showed higher engineering efficiency. The five main mechanical properties of each specimen are listed in Table 3: Von Mises Stress: This

composite metric, which shows the total amount of stress in the body, is a crucial indicator of the start of yielding. The maximum shear stress that a material experiences as a result of loading is expressed by this term. The stress intensity at the critical point, which is quite near to the von Mises stress, is shown by this metric. The amount of elastic deformation a material can withstand before failing is indicated by its corresponding elastic strain. Equivalent elastic stress is the expression of the equivalent stress value inside the elastic limit.

Table 3. Comparative statistical analysis of stress and strain values in the eight models

Models	Von Miss Stress (Mpa)	Maximum Shear Stress (Mpa)	Stress Intensity (Mpa)	Equivalent Elastic Strain (mm/mm)	Equivalent Elastic Stress (Mpa)
I	465.21	233.05	466.10	0.00647	466.78
II	424.66	212.79	424.79	0.00591	426.24
III	392.96	201.71	403.42	0.00548	398.47
IV	357.9	183.52	367.04	0.00499	363.72
V	465.38	233.11	466.22	0.00225	466.91
VI	424.62	212.34	424.68	0.002205	426.16
VII	443.67	222.9	445.79	0.00215	447.04
VIII	358.55	183.8	367.60	0.00174	364.83

Comparing steel and AA7075-T6 aluminum alloy, the von-Meis stress of aluminum is approximately 3% higher than that of steel, indicating a superior capacity to withstand equivalent stresses. The variability within aluminum specimens is also relatively lower than that of steel, while steel exhibits a gradual stress decrease of approximately 23% from specimen I to IV, reflecting a clear influence of the hole distribution or specimen arrangement on the stress distribution.

Although the pattern of reduction from maximum to minimum is comparable in both materials (~21%), the average shear stresses in aluminum are somewhat higher (~2.5%) than in steel. The findings show that while the geometric distribution had a similar effect on shear stress in both alloys, AA7075-T6 aluminum showed 9% more stability and a 7.3% decrease in stress intensity when compared to steel. With a more consistent strain distribution and a 61.5% decrease in elastic strain as opposed to 22.9% for steel, aluminum showed greater resilience to deformation. According to studies [55, 56], aluminum is 60–70% more elastic and ductile than steel, which improves its capacity to distribute and absorb stress. Due to their sensitivity to geometric design, steel models exhibited substantial variability (21–23%), while aluminum models only displayed 4–5%. Aluminum's greater rigidity, elasticity, and balanced stress-strain distribution can be explained by this. As a result, aluminum offers more consistent mechanical performance while steel shows more variability. Aluminum may minimize the variation in internal stress intensity and distribute stress more equally among models because of its greater ductility, lighter weight, and lack of rigidity. Geometric Openings and Distribution's Effect: Differences in the arrangement or shape of apertures between models have an effect on stress concentration. The concentration is higher and the stress intensity between the maximum and minimum points decreases more because steel is less ductile. Aluminum can effectively distribute stress around the holes due to its ductility, which lowers internal stress.

Stiffness and Deformation Interaction: Steel exhibits less deformation per stress level, but every change in shape or opening causes notable variations in stress intensity (variance ≈ 21%). Aluminum has a higher strain but a more uniform stress distribution, resulting in a smaller fluctuation (≈ 9%). The main causes of the discrepancy are the various material characteristics (stiffness and elasticity) and the impact of the engineering design on the distribution of stress. Steel is more rigid, thus there are more differences in stress intensity between models, whereas aluminum is more elastic, so the stress is more evenly distributed. Because aluminum exhibits more ductile behavior at low temperatures and high rates of deformation, the study suggests that aluminum has a greater capacity for deformation than steel [57]. Furthermore, both studies show that because aluminum deforms more quickly and has a lower temperature ductility than steel, it has a greater capacity for deformation [42, 43].

6. CONCLUSIONS

The most important conclusions reached by this study can be drawn based on the results that were accurately and comprehensively measured and analyzed. The data and experiments conducted demonstrated the extent of the interrelationship between the studied factors and their direct impact on the overall performance of the system or material under investigation. Through data analysis and discussion of the results, it was possible to identify the most important points that reflect the effectiveness of the methodology used and the accuracy of the analytical methods in arriving at clear indicators that support the study's objectives and confirm the validity of the proposed hypotheses. Based on this, it can be said that these conclusions represent a reliable scientific conclusion that contributes to clarifying the behavior of the model studied and opens new horizons for future research in the same field.

1. According to simulation results, symmetrical hole placement reduces stress in both alloys. Model IV has the lowest concentration and most efficient stress dispersion, as seen by the continuous rise in stress reduction for AISI 4130 steel from Model II (~8.7%) to Model IV (~23.1%). For the aluminum alloy AA7075-T6, Models VI and VII exhibit moderate reductions (~4.7–8.7%), whereas Model VIII is the most efficient configuration for lowering stress concentration (~22.9%). The finest models for steel and aluminum overall are Model IV and Model VIII, which

exhibit improved mechanical performance and stress homogeneity under static loading circumstances.

2. The results showed that in both alloys, symmetrical hole distribution considerably decreased maximum shear stress. In AISI 4130 steel, the fourth pattern produced a uniform distribution of stress and the largest decrease (21.3%). The eighth design, which reduced by about 21.1%, was the most effective in AA7075-T6 aluminum. Geometrically symmetric designs are therefore perfect for increasing mechanical stability and reducing concentrations. The most effective motifs are the fourth and eighth.
3. Stress intensity was significantly reduced in both alloys when the hole distribution was altered. Steel alloys had the largest reduction of around 20.5% (model 8 compared to model 5), reflecting the general trend of improvement, while aluminum alloys had the highest stress dissipation efficiency with a reduction of over 22% (model 4 compared to model 1). In terms of reducing stress concentration, aluminum alloys performed 1.5% better than steel, suggesting a greater sensitivity to hole distribution and enhanced capacity for dissipating stress.
4. Aluminum alloys outperformed steel in reducing strain concentration by more than 1.5% under the identical loading and geometrical conditions. This is explained by their increased ductility and sensitive responsiveness to hole distribution, which helped to reduce localized strains more effectively. Because of its relative stiffness, steel showed a reduced ability to absorb and dissipate strain despite its great strength.
5. The numerical analysis revealed a considerable improvement in stress uniformity along with a progressive drop in the ultimate strain values in aluminum alloys from model (1) to model (4). Model (4) fared better than model (1) by almost 30%, indicating a rise in deformation resistance and mechanical efficiency. The enhanced model (VIII) design for steel resulted in a 23% decrease in strain and better stress uniformity, which raised structural efficiency by about 25%.
6. The average equivalent stress in steel was 466.78 ± 25.9 MPa, whereas in aluminum it was 466.91 ± 18.2 MPa, according to descriptive statistical studies, indicating that aluminum had greater statistical stability and less stress dispersion. Additionally, aluminum's stress levels dropped by 11.6% (±7.9%) while steel's reduced by 15.1% (±5.8%), suggesting that steel had more variability. Steel was more affected by geometric change, while aluminum was more stable and had a more uniform stress distribution, according to the ANOVA results, which also indicated significant differences between the models ($p < 0.05$).
7. As a result of design optimization, the aluminum alloy's maximum stress dropped by 22.5%, from 466.78 MPa to 361.72 MPa. In contrast, the steel alloy's stress levels decreased from 446.51 MPa to 363.45 MPa, which is an 18.6% decrease and indicates a notable improvement in load distribution. Compared to steel, aluminum showed a higher stress reduction rate of about 3.9%, suggesting that it responds to engineering changes more effectively. Furthermore, despite the lower percentage increase, steel showed stronger absolute stability because of its greater stiffness. Therefore, it may be said that steel is more mechanically stable under the same loading conditions, while aluminum is more susceptible to engineering modifications.
8. The investigation discovered that the addition of side holes to the second and third samples of the aluminum alloy AA7075-T6 increased the safety margin from 87% to 91-92% by lowering the von Mises stress from 465 MPa to about 430-440 MPa. The safety margin rose to 85–87% and the stress decreased from 223 to 190–200 MPa under the maximum shear hypothesis. In the AISI 4130 steel alloy, the revised design in the sixth and seventh samples lowered stress from 465 to around 425-440 MPa, increasing the safety margin to 87-88%. The safety margin under the shear theory has also improved from 74% to 78-80%. The comparison shows that the side apertures considerably improved stress distribution, increasing the structural integrity of both materials.
9. The mechanical performance of both AISI 4130 steel and AA7075-T6 aluminum was significantly improved by optimizing the perforation design. Because to the better perforation form and size, the ultimate stress concentration dropped by 15–22% in aluminum and 18–25% in steel. The efficiency of the enhanced design was demonstrated by the 10% and 13% increases in load-bearing capacity prior to yielding in aluminum and steel, respectively. Additionally, overall deformation was reduced by 11% for steel and 9% for aluminum, improving structural stability. These findings show that improving mechanical characteristics and structural performance without raising production costs can be achieved by optimizing perforation sites and shapes.

7. SUGGESTIONS AND FUTURE STUDIES

These recommendations and future studies could be directly related to the research findings, expanding the area of future work:

1. Instead of relying solely on static loading, a simulation study employing dynamic and variable loads is proposed to examine the effect of hole distribution on material strength under real-world conditions.
2. Examining the effects of other materials: To comprehend how mechanical properties and ductility affect stress distribution and reduction, compare the behavior of light alloys or composites (such as Mg or Ti alloys) to aluminum and steel.
3. Analyzing the impact of altering sheet thickness or constructing non-circular holes (e.g., oval, square, or with diameter gradients) on stress distribution and structural stiffness.
4. Validate ANSYS simulation results by conducting experiments on similar models, especially for aluminum models with higher hole distribution sensitivity.
5. Optimizing statistical distribution parameters: Using advanced statistical analysis (e.g., Monte Carlo or sensitivity analysis) to assess how modest geometric changes affect mechanical stability and ultimate strain in each model.
6. Multi-objective optimization involves combining stress reduction, structural stiffness increase, and weight reduction utilizing evolutionary algorithms or artificial intelligence to discover the best hole arrangement and number.
7. Analyzing stress and strain distribution in aluminum-steel and polymer/metallic composites to optimize mechanical

distribution and design more efficient structures.

REFERENCES

[1] Pirkle, M.K., Mallick, P.K. (2025). A numerical study of the effect of hole offset on stress concentrations due to a square hole in a quasi-isotropic composite laminate. Journal of Composites Science, 9(6): 286. https://doi.org/10.3390/jcs9060286

[2] Jain, N. (2011). The reduction of stress concentration in a uni-axially loaded infinite width rectangular isotropic/orthotropic plate with central circular hole by coaxial auxiliary holes. IIUM Engineering Journal, 12(6): 141-150. https://doi.org/10.31436/iiumej.v12i6.228

[3] Lin, X., Zhang, L., Xie, Y. (2025). Research on the stress concentration effects and fracture mechanisms of DC04 sheet steel with holes. Frontiers in Materials, 12: 1488624. https://doi.org/10.3389/fmats.2025.1488624

[4] Miller, B., Maksymovych, M., Maksymovych, O., Gagauz, F. (2025). Optimization of stresses near reinforced holes in relation to sustainable design of composite structural elements. Sustainability, 17(15): 7103. https://doi.org/10.3390/su17157103

[5] Ali, H.M., Najem, M.K., Karash, E.T., Sultan, J.N. (2023). Stress distribution in cantilever beams with different hole shapes: A numerical analysis. International Journal of Computational Methods and Experimental Measurements, 11(4): 205-219. https://doi.org/10.18280/ijcmem.110402

[6] Meguid, S.A. (1986). Finite element analysis of defence hole systems for the reduction of stress concentration in a uniaxially-loaded plate with two coaxial holes. Engineering Fracture Mechanics, 25(4): 403-413. https://doi.org/10.1016/0013-7944(86)90254-7

[7] Endigeri, B.R., Mannur, D.V. (2014). FEM for stress reduction by optimal auxiliary holes in a uniaxially loaded composite plate. In Proceedings of International Conference on Research in Electrical, Electronic and Mechanical Engineering, Dehradun.

[8] Ali, H.M., Najem, M.K., Karash, E.T., Sultan, J.N. (2023). Stress distribution in cantilever beams with different hole shapes: A numerical analysis. International Journal of Computational Methods and Experimental Measurements, 11(4): 205-219. https://doi.org/10.18280/ijcmem.110402

[9] Abdalla, H.M.A., De Bona, F., Casagrande, D. (2025). Stress concentration optimization for functionally graded plates with noncircular holes. Computers & Structures, 315: 107792. https://doi.org/10.1016/j.compstruc.2025.107792

[10] Dai, Y., Chen, J., Yu, C., Almutairi, A.D., Yuan, Y. (2025). Comparative analysis of strength improvement techniques in perforated glass fiber reinforced polymer plates: Adhesive filling, bolt reinforcement, and elliptical perforation design. Materials, 18(18): 4290. https://doi.org/10.3390/ma18184290

[11] Suzuki, S.I. (1969). Stress measurements in an infinite plate with a hole reinforced by different materials: Relationships between stress-concentration factors, the ratio of Young's moduli of a plate and rings, and dimensions of rings are studied. Experimental Mechanics, 9(7): 332-336. https://link.springer.com/article/10.1007/BF02325140.

[12] Burjes, A.Y., Sulaiman, A.A., Najm, H.Y. (2022). Stress study by the finite element analysis of a plate with a central hole. Journal of Global Scientific Research, 7(8): 2542-2549. https://doi.org/10.5281/zenodo.7023016

[13] Liu, H., Deng, L., Wang, W. (2024). 3D stress concentration around circular hole under remote biaxial loading. International Journal of Mechanical Sciences, 268: 109032. https://doi.org/10.1016/j.ijmecsci.2024.109032

[14] Wu, F., Zhang, Y., Zhao, B., Ren, Y., Yan, J. (2025). Shear performance of PBL shear connectors under combined bending-shear loading: Experimental and numerical studies. Case Studies in Construction Materials, 23: e05326. https://doi.org/10.1016/j.cscm.2025.e05326

[15] Sivák, P., Delyová, I., Bocko, J. (2023). Comparison of stress concentration factors obtained by different methods. Applied Sciences, 13(24): 13328. https://doi.org/10.3390/app132413328

[16] Kaya, S., Sonmez, F.O. (2025). Optimum local reinforcements for maximum strength of composite plates with a cutout. Structural and Multidisciplinary Optimization, 68(7): 128. https://doi.org/10.1007/s00158-025-04041-8

[17] Kubair, D.V., Bhanu-Chandar, B. (2008). Stress concentration factor due to a circular hole in functionally graded panels under uniaxial tension. International Journal of Mechanical Sciences, 50(4): 732-742. https://doi.org/10.1016/j.ijmecsci.2007.11.009

[18] Shahriar, A., Majlesi, A., Montoya, A. (2024). Modeling holes and voids in three dimensions using a single element within the extended finite element framework. International Journal for Computational Methods in Engineering Science and Mechanics, 25(2): 56-79. https://doi.org/10.1080/15502287.2023.2274025

[19] Levin, V.A., Zingerman, K.M., Vershinin, A.V., Freiman, E.I., Yangirova, A.V. (2013). Numerical analysis of the stress concentration near holes originating in previously loaded viscoelastic bodies at finite strains. International Journal of Solids and Structures, 50(20-21): 3119-3135. http://doi.org/10.1016/j.ijsolstr.2013.05.019

[20] Younis, N.T. (2006). Assembly stress for the reduction of stress concentration. Mechanics Research Communications, 33(6): 837-845. https://doi.org/10.1016/j.mechrescom.2006.03.007

[21] Fuad, K., Siregar, R.A., Rangkuti, C., Ariwahjoedi, B., Firdaus, M. (2007). Stress concentration factors of various adjacent holes configurations in a spherical pressure vessel. In Proceedings of the 5th Australasian Congress on Applied Mechanics, ACAM 2007, Brisbane, Australia, pp. 68-73. https://search.informit.org/doi/10.3316/informit.217831788002647.

[22] Karash, E.T., Ali, H.M., Kassim, M.T.E. (2024). Designing cantilever models from various materials and comparing them when they are under constant load and have holes. Revue des Composites et des Materiaux Avances, 34(3): 363-377. https://doi.org/10.18280/rcma.340312

[23] Aiad, S.M., Enab, T.A., Aboueleaz, M.A. (2023). Analysis of stress and strain concentrations around an elliptical hole via finite element and response surface methodology. Mansoura Engineering Journal, 49(3): 3.

https://doi.org/10.58491/2735-4202.3175
[24] Abdalla, H.M.A., Casagrande, D., De Bona, F. (2023). Analysis of stress concentration in functionally graded plates with linearly increasing Young's modulus. Materials, 16(21): 6882. https://doi.org/10.3390/ma16216882
[25] Hart, E.L., Terokhin, B.I. (2025). Effect of functionally graded inclusion on stress conservation near a circular hole in thin plates for different boundary conditions. Journal of Optimization, Differential Equations and Their Applications, 33(1): 110-127. https://doi.org/10.15421/142506
[26] Qi, C., Zhao, Y., Yang, X., Xie, Y., Yu, X., Gai, J., Meng, Z., Zhai, S., Gong, R. (2025). Scattering and dynamic stress concentration analysis of elastic waves around arbitrarily shaped holes in piezoelectric smart building materials. Scientific Reports, 15(1): 31692. https://doi.org/10.1038/s41598-025-16974-7
[27] Wang, W., Yuan, H., Li, X., Shi, P. (2019). Stress concentration and damage factor due to central elliptical hole in functionally graded panels subjected to uniform tensile traction. Materials, 12(3): 422. https://doi.org/10.3390/ma12030422
[28] Goyat, V., Verma, S., Garg, R.K. (2019). Stress concentration reduction using different functionally graded materials layer around the hole in an infinite panel. Strength, Fracture and Complexity, 12(1): 31-45. https://doi.org/10.3233/SFC-190232
[29] Konieczny, M., Achtelik, H., Gasiak, G. (2020). Stress distribution in a plate with a hole along the diagonal distribution under plane biaxial load. Strojnicky Casopis, 70(2): 91-100. https://doi.org/10.2478/scjme-2020-0023
[30] Elsherbiny, A.A., Enab, T.A., Eladl, A. (2025). Incremental metal forming of functionally graded aluminum-copper composites: A numerical investigation by finite element analysis. Mansoura Engineering Journal, 50(4): 12. https://doi.org/10.58491/2735-4202.3296
[31] Zhao, T.Y., Jiang, L.P., Yu, Y.X., Wang, Y.Q. (2023). Study on theoretical modeling and mechanical performance of a spinning porous graphene nanoplatelet reinforced beam attached with double blades. Mechanics of Advanced Materials and Structures, 30(8): 1530-1541. https://doi.org/10.1080/15376494.2022.2035862
[32] Afolabi, S.O., Oladapo, B.I., Ijagbemi, C.O., Adeoye, A.O., Kayode, J.F. (2020). Design and finite element analysis of fatigue life prediction for safe and economical machine shaft. Journal of Materials Research and Technology, 8(1): 105-111. https://doi.org/10.1016/j.jmrt.2017.10.007
[33] Li, Z., Dai, W., Yue, H., Guo, C., Ji, Z., Li, Q., Zhang, J. (2025). Fatigue life prediction of 2024-T3 clad Al alloy based on an improved SWT equation and machine learning. Materials, 18(2): 332. https://doi.org/10.3390/ma18020332
[34] Bertolini, R., Simonetto, E., Pezzato, L., Fabrizi, A., Ghiotti, A., Bruschi, S. (2021). Mechanical and corrosion resistance properties of AA7075-T6 sub-zero formed sheets. The International Journal of Advanced Manufacturing Technology, 115(9): 2801-2824. https://doi.org/10.1007/s00170-021-07333-7
[35] Emmanuel, O.K., Nwawe Tchadeu, R., Marashi Najafi, F., Madani, S., Chizari, M. (2024). Failure strength of 7075-T6 aluminium alloy: Integrating digital image and finite element analysis for static uniaxial and biaxial load scenarios. Journal of Design Against Fatigue, 2(2): 13-21. https://doi.org/10.62676/jdaf.2024.2.2.20
[36] AZoM. (2001). AISI 4130 Alloy Steel (UNS G41300). https://www.azom.com/article.aspx?ArticleID=6742.
[37] Aluminum 7075-T6. MatWeb material property data. https://asm.matweb.com/search/specificmaterial.asp?bassnum=ma7075t6.
[38] Dou, S., Liu, Z., Li, Z., Shi, H., Zhou, K., Xia, J. (2025). Mechanical properties of 7075-T6 aluminum alloy in electrically assisted forming. Metals, 15(2): 117. https://doi.org/10.3390/met15020117
[39] Chen, C., Feng, L. (2025). Effect of geometrical configuration and strain rate on aluminum alloy 5083 and S550 steel characterized by digital image correlation. Sensors, 25(12): 3607. https://doi.org/10.3390/s25123607
[40] Gharaibeh, M.A. (2020). A study on the stress concentration factor induced in double countersunk holes due to uniaxial tension. International Journal of Applied Mechanics and Engineering, 25(4): 59-68. https://doi.org/10.2478/ijame-2020-0049
[41] Badiger, S., DS, R. (2023). Stress distribution in an infinite plate with discontinuities like elliptical or circular hole by boundary force method. SN Applied Sciences, 5(3): 77. https://doi.org/10.1007/s42452-023-05289-9
[42] Esmaeili, J., Asgharpour, A., Bakhshi-Jooybari, M., Gorji, H., Mirnia, M.J. (2025). Experimental and numerical study of forming aluminum stepped tubes by electromagnetic forming method. Discover Materials, 5(1): 138. https://doi.org/10.1007/s43939-025-00337-0
[43] Konieczny, M., Gasiak, G., Achtelik, H. (2021). Influence of the applied layer on the state of stress in a bimetallic perforated plate under two load variants. Fracture and Structural Integrity, 15(56): 137-150. https://doi.org/10.3221/IGF-ESIS.56.11
[44] Bulut, N.Z.C., Özkan, M.T., Ozdemir, V. (2025). FEM and ANN modeling of stress concentration factors (K_t) of circular plates with various circular holes according to internal and external pressures. Materials Testing, 67(10): 1591-1612. https://doi.org/10.1515/mt-2025-0139
[45] Kadir, R.A., Abdullah, S., Yusuf, A.M., Isa, K.M., Arhafudin, A.M. (2023). Comparative analysis of aluminum and steel mechanical properties. Marine Frontier, 14(2): 27-31.
[46] Uematsu, Y., Ozeki, Y., Toasa Caiza, P.D. (2023). Tensile-shear properties of steel-Al adhesively bonded dissimilar joints and the effect of Al plate thickness. Scientific Reports, 13: 19819. https://doi.org/10.1038/s41598-023-47072-1
[47] Radhakrishnan, G., Breaz, D., Al Khusaibi, S.S., Al Subaihi, A.J., Al Ismaili, A.A.Z., AlMaani, A.M., Karthikeyan, K.R. (2023). Experimental and numerical study on the influence of stress concentration on the flexural stability of an aluminium hollow tube. Materials, 16(4): 1492. https://doi.org/10.3390/ma16041492
[48] Izard, E., García-Martín, R., Rodríguez-Martín, M., Lorenzo, M. (2023). Finite element analysis of the influence of chamfer hub geometry on the stress concentrations of shrink fits. Applied Sciences, 13(6): 3606. https://doi.org/10.3390/app13063606
[49] Yang, Q., Gao, C., Chen, W. (2012). Stress concentration

in a finite functionally graded material plate. Science China Physics, Mechanics and Astronomy, 55(7): 1263-1271. https://doi.org/10.1007/s11433-012-4774-x

[50] Tang, T., Wang, L., Zhu, M., Zhang, H., Dong, J., Yue, W., Xia, H. (2024). Topology optimization: A review for structural designs under statics problems. Materials, 17(23): 5970. https://doi.org/10.3390/ma17235970

[51] Giraldo-Londoño, O., Russ, J.B., Aguiló, M.A., Paulino, G.H. (2022). Limiting the first principal stress in topology optimization: A local and consistent approach. Structural and Multidisciplinary Optimization, 65(9): 254. https://doi.org/10.1007/s00158-022-03320-y

[52] Abdalla, H.M.A., De Bona, F., Casagrande, D. (2024). Optimization of functionally graded materials to make stress concentration vanish in a plate with circular hole. Composites Part C: Open Access, 15: 100512. https://doi.org/10.1016/j.jcomc.2024.100512

[53] Guo, W., Guo, W. (2019). Formulization of three-dimensional stress and strain fields at elliptical holes in finite thickness plates. Acta Mechanica Solida Sinica, 32: 393-430. https://doi.org/10.1007/s10338-019-00091-w

[54] You, H., Zhang, L., Lin, X., Tang, P., Du, Q. (2025). Stress concentration characteristics and coefficient modification for DC04 steel with holes of finite thickness. Frontiers in Materials, 12: 1692324. https://doi.org/10.3389/fmats.2025.1692324

[55] Ghoujehzadeh, A., Mohtadi-Bonab, M.A., Jahani, D. (2025). Optimization and finite element analysis of an aluminum piston in the Peugeot XU7JPL3 engine for enhanced efficiency and durability. Discover Mechanical Engineering, 4(1): 6. https://doi.org/10.1007/s44245-025-00091-w

[56] Li, D., Wu, F., Cai, Z., Almutairi, A.D., Zhou, J., Dai, Y. (2025). Stress concentration in glass fiber reinforced polymer plates induced by central circular holes and bolted connections. Case Studies in Construction Materials, 23: e05356. https://doi.org/10.1016/j.cscm.2025.e05356

[57] Jabri, A.A., Gharaibeh, M.A. (2025). Investigation of stress concentration factors in countersunk holes of biaxially loaded isotropic plates. International Journal of Applied Mechanics and Engineering, 30(1): 79-88. https://doi.org/10.59441/ijame/197486